

## AFFECTING PARAMETERS TO THE HEAT AND MASS TRANSFER OF NH<sub>3</sub>-H<sub>2</sub>O SOLUTION FALLING ON THE HORIZONTAL ROUND TUBE

NGUYEN HIEU NGHIA <sup>1</sup>, LE CHI HIEP <sup>2</sup>, DUONG CONG TRUYEN <sup>1</sup>

<sup>1</sup>Faculty of Heat & Refrigeration Engineering, Industry University of Ho Chi Minh City,

<sup>2</sup>Department of Heat & Refrigeration Engineering, Ho Chi Minh City University of Technology, VNU-HCM;

nguyenhieunghia@iuh.edu.vn

**Abstract.** The absorption process has been confirmed as the most important process in absorption refrigeration machines in terms of improving their total efficiency. One of the key research directions is the selection of absorber structure which is expected to be fabricated in Vietnam without demand of new infrastructure investment. In this study, a local model of the coupled heat and mass transfer during absorption process of NH<sub>3</sub> vapor by a NH<sub>3</sub>-H<sub>2</sub>O diluted solution flowing over horizontal round tubes of an absorber was made. The heat transfer coefficient obtained from the coupled heat and mass transfer mathematic model. This heat transfer coefficient is used to calculate the variation of the simulated value of heat load. The correlations which give the heat transfer coefficient and mass transfer coefficient in the absorption process in range of solution concentration  $\omega = 28\% \div 31\%$ , solution mass flow rate per unit tube length  $\Gamma = 0.001 \div 0.03 \text{ kgm}^{-1}\text{s}^{-1}$ , coolant temperature  $t_{\text{water}} = 28 \text{ }^\circ\text{C} \div 38 \text{ }^\circ\text{C}$  are set as two functions. The practical decrease of wetted ratio analyses were taken into account when the solution flow from the top to the bottom of the parallel tube bundle. The deviation of theoretical heat load and experimental heat load is about 12.3%. Based on these simulations, the theoretical studies were done for absorption refrigeration system in order to narrow the working area where the experiments later focused on. The results of this study will be the basis for subsequent application research of falling film absorbers.

**Keywords.** Absorption process, NH<sub>3</sub>-H<sub>2</sub>O solution, falling film, absorption refrigeration.

### Nomenclature

x	Tangential coordinate along solution flow direction, m
y	Local radial coordinate normal to solution flow direction, m
$\varepsilon$	Non-dimensional tube half-circumference
$\eta$	Non-dimensional film thickness
u	Circumferential velocity, $\text{ms}^{-1}$
v	Normal velocity, $\text{ms}^{-1}$
$\delta$	Film thickness, m
$\omega$	Solution concentration
T	Temperature, K
h	Enthalpy, $\text{kJkg}^{-1}$
$\Gamma$	Solution mass flow rate per unit length, $\text{kgm}^{-1}\text{s}^{-1}$
$\alpha_{ib}$	Convective heat transfer coefficient from interface to bulk, $\text{Wm}^{-2}\text{K}^{-1}$
$\alpha_{bw}$	Convective heat transfer coefficient from bulk to wall, $\text{Wm}^{-2}\text{K}^{-1}$
$\alpha_{iw}$	Heat transfer coefficient from interface to wall, $\text{W m}^{-2}\text{K}^{-1}$
$\alpha_w$	Convective heat transfer coefficient of cooling water, $\text{Wm}^{-2}\text{K}^{-1}$
U	Heat transfer coefficient from film to water, $\text{Wm}^{-2}\text{K}^{-1}$
$h_m$	Mass transfer coefficient from interface to bulk, $\text{ms}^{-1}$
$\nu$	Kinetic viscosity $\text{m}^2\text{s}^{-1}$
WR	Wetted ratio, %
$\theta$	Angle, radian
m	Mass flow rate, $\text{kgs}^{-1}$
$D_o$	Outer diameter of the tube, mm

$D_i$	Inner diameter of the tube, mm
$q_f$	Heat flow rate, $Wm^{-2}$
$m_f$	Mass flow rate, $kgm^{-2}s^{-1}$
$Q$	Heat load, kW

## 1 INTRODUCTION

The performance of the absorption refrigeration system depends on the absorber. Heat and mass transfer processes occurring between liquid and vapor phases are key points in sizing and designing the absorber [1], [2]. The falling film absorbers include the following main types: 1. The falling films flow on two cooling walls. In wall structure, the mass transfer efficiency of the bubble form is better than of the falling film form. 2. The falling films flow over the circular wall. 3. Dilute NH<sub>3</sub> solution from the dispenser is sprayed onto horizontal tubes which are arranged unequal. 4. The tubes are arranged parallel and connected with the grid for increasing the contacting surface. 5. Dilute NH<sub>3</sub> solution from a dispenser dispensed onto parallel tubes was selected because of its simple structure, good heat transfer performance, and can be fabricated according to the existing technology conditions in Vietnam that is no need to import new production lines. This research focuses on the coupled heat and mass transfer of falling film absorption on the horizontal tubes of the cooling tube bundle. Heat transfer coefficient, mass transfer coefficient, the distribution of solution concentration profile and temperature profile of the film leaving the bottom cooling tube having decisive role in appropriate choice between adequate size of absorbers design and system operation. Moreover, falling film absorber is the most popular due to many advantages of heat transfer efficiency, easy to assemble, easy to manufacture, especially well-suited to the technology conditions in Vietnam. Therefore, the study of absorption properties of the falling film and parameters influencing on heat transfer coefficient and mass transfer coefficient of the absorption process are urgently needed for design, manufacture, and operation.

Two common pairs of working fluid (refrigerant-absorbent) of refrigeration absorption systems are H<sub>2</sub>O-LiBr and NH<sub>3</sub>-H<sub>2</sub>O. Testing absorber is using dilute NH<sub>3</sub>-H<sub>2</sub>O solution concentration distributed evenly from top to form the falling film around the tubes of parallel tube layers, NH<sub>3</sub> vapor go pass through the tube layers from the absorber bottom [4] ÷ [9]. Dilute solution absorb NH<sub>3</sub> vapor to become stronger solution generating the absorbing heat flow. This heat flow go through the tube wall to the cooling water flowing in tubes and carrying it away. The falling film covers only one part of the tube depends on the fluid distribution along the tube length and surface tension of the solution, as well as surface roughness of tube.

## 2 MATHEMATICAL MODEL

### 2.1 Model description

The structure and the arrangement of the flows in the absorber: A tube bundle consists of the horizontal tube rows stacked on a vertical axis. The diluted NH<sub>3</sub>-H<sub>2</sub>O solution flow and NH<sub>3</sub> vapor flow are in the opposite directions. The tube diameter is  $\Phi 9.6$  mm, the vertical step is 20 mm and the horizontal step is 13 mm

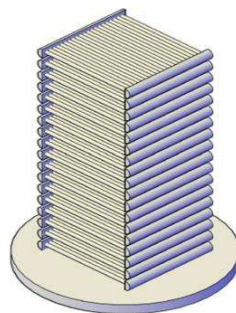


Figure 1: The structure of the selected falling film absorber

Each cooling tube is divided into k control volume elements. After leaving the control volume element of the upper tube, NH<sub>3</sub>-H<sub>2</sub>O solution enters to the next below control volume element of the next below tube with the same temperature and concentration profiles during leaving the previous element. Once the cooling water temperature enters the absorber is known, the calculation method will be started with each control element. This procedure continues until the entire tube length is finish. The next progress for the next tube model is repeated until the last tube is finished. The cooling water temperature calculation leaves the absorber will be compared with experimental value. If the deviation exceeds the allowable value, the entire calculation process is repeated with a new value of the cooling water may be anticipated until the calculation converges.

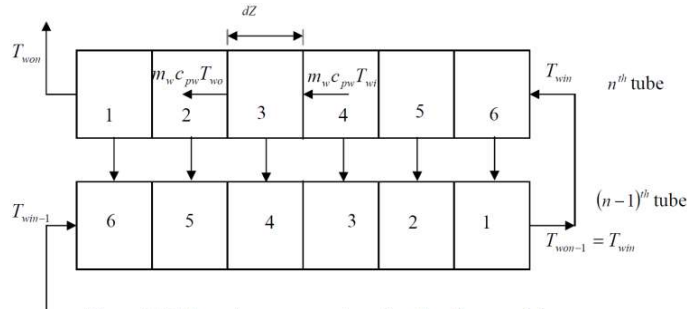


Figure 2: Spatial discretization of falling film solution

A control volume element has 100% wetted ratio. 3D physical models become 2D physical model has dilute solution flow direction along the tube circumference by coordinate x. Film thickness direction is from the tube center by coordinate y. Any points on the film are determined by coordinate  $\theta$ , y respectively.

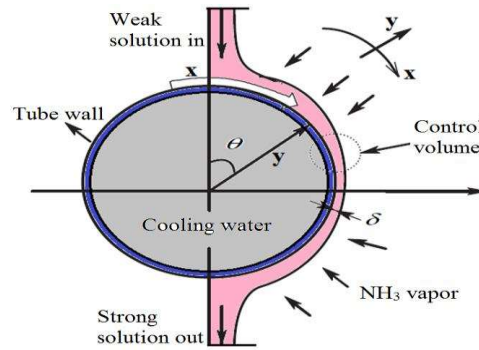


Figure 3: 2D physical model

## 2.2 Mathematical description

The continuity, momentum, energy, transport equations of the solution falling film on the tube bundle are described 2D [2] ÷ [13].

For a given solution mass flow rate per unit tube length  $\Gamma = \dot{m}/L$ . Film thickness is expressed as equation (1).

$$\delta = \left[ 1 - \frac{3v\Gamma}{(WR)\rho g \sin\theta} \right]^{1/3} \quad (1)$$

The velocity component u along x direction is belong to flow direction as equation (2).

$$u = \frac{g \sin\theta}{2v} (2\delta y - y^2) \quad (2)$$

The velocity component v along y direction is normal to flow direction as equation (3).

$$v = -\frac{g}{2v} y^2 \left[ \frac{d\delta}{dx} \sin\theta + \frac{1}{R_o} \left( \delta - \frac{y}{3} \right) \cos\theta \right] \quad (3)$$

The phenomenon of coupled heat and mass transfer in steady state is described by the energy transport

equation (4) and the species transport equation (5).

$$u \frac{\partial T}{\partial x} + v \frac{\partial T}{\partial y} = \alpha \frac{\partial^2 T}{\partial y^2} \quad (4)$$

$$u \frac{\partial \omega}{\partial x} + v \frac{\partial \omega}{\partial y} = D \frac{\partial^2 \omega}{\partial y^2} \quad (5)$$

Concentration and temperature boundary conditions at the inlet (6).

$$\begin{cases} x = x_{in} \\ 0 \leq y \leq \delta \end{cases} \rightarrow \begin{cases} T = T_{in} \\ \omega = \omega_{in} \end{cases} \quad (6)$$

Concentration and temperature boundary conditions on the tube wall surface (7).

$$\begin{cases} x_{in} \leq x \leq x_{out} \\ y = 0 \end{cases} \rightarrow \begin{cases} T = T_{wall} \\ \frac{\partial \omega}{\partial y} = 0 \end{cases} \quad (7)$$

Concentration and temperature boundary conditions at the liquid-vapor interface (8, 9, 10).

$$\begin{cases} x_{in} \leq x \leq x_{out} \\ y = \delta \end{cases} \rightarrow \begin{cases} \dot{m} = \frac{\rho D}{(1 - \omega_{int})} \frac{d\omega}{dy} \text{ at } y = \delta \text{ (concentration)} \quad (8) \\ q = m' h_{ab} = k_f \frac{dT}{dy} \text{ at } y = \delta \text{ (heat flow)} \quad (9) \\ T_{int} = f(p, \omega_{int}) \text{ at } y = \delta \text{ (equivalent)} \quad (10) \end{cases}$$

The local heat transfer coefficients from the interface to bulk solution along the film flow (11) and from the bulk solution to tube wall surface along the film flow (12) in terms of Nusselt number.

$$Nu_{ib} = \frac{\alpha_{ib} \delta}{k_f} = \frac{\delta}{(T_{int} - T_{sb})} \frac{dT}{dy} \text{ at } y = \delta \quad (11)$$

$$Nu_{bw} = \frac{\alpha_{bw} \delta}{k_f} = \frac{\delta}{(T_{sb} - T_w)} \frac{dT}{dy} \text{ at } y = 0 \quad (12)$$

The mass transfer coefficient from the interface to bulk solution along the film flow (13) in terms of Sherwood number.

$$Sh = \frac{h_m \delta}{D_{ab}} = \frac{m' \delta}{D_{ab} \rho (\omega_{int} - \omega_{sb})} \quad (13)$$

The heat transfer coefficient from the interface to cooling water flow can be expressed as (14) [2], [3].

$$\frac{1}{U} = \frac{1}{\alpha_{iw}} + \frac{1}{\alpha_w} + \frac{\delta_{wall}}{\lambda_{wall}} \quad (14)$$

The physical domain has a complex geometry. Moreover, the film thickness is in micro-size vs the half circumference length 0.0157 m. This ratio make the domain can not be meshed directly which must be transformed from sliding coordinate  $xy$  to non-dimensional coordinate  $\epsilon\eta$  making the computational domain rectangular.

The counter-flow absorber is presented schematically as shown in figure 2. Applying the conservation law of energy to the control volume element, the following equations are obtained (figure 3):

Heat load removed on the coolant flow for a control volume element, W

$$Qdz = m_w c_{pw} \cdot dT_w \quad (15)$$

The outer wall temperature of a control volume element, °C

$$T_{wall,o} - T_w = m_w c_{pw} \left[ \frac{1}{i_w \pi D_i} + \frac{\ln(D_o/D_i)}{2\pi k_{wall}} \right] \frac{dT_w}{dz} \quad (16)$$

$$T_{w,k} = \frac{T_{wi} + T_{wo}}{2} \quad (17)$$

$$dT_w = T_{wo} - T_{wi} \quad (18)$$

$$T_{wall,o} = \frac{T_{w,k} - T_{w,k+1} \exp \left[ dz \left\{ m_w c_{pw} \left( \frac{\ln(D_o/D_i)}{2\pi k_{wall}} + \frac{1}{i_w \pi D_i} \right) \right\} \right]}{1 - \exp \left[ dz \left\{ m_w c_{pw} \left( \frac{\ln(D_o/D_i)}{2\pi k_{wall}} + \frac{1}{i_w \pi D_i} \right) \right\} \right]} \quad (19)$$

The heat flux transferred into a control volume element, W:

$$dA * q_f = dA * (m' i_{ab}) = dA * \left( k_f \frac{dT}{dy} \right) \quad (20)$$

The absorber head load, W

$$Q_f = q_f * A \quad (21)$$

The absorber mass flow rate,  $\text{kg s}^{-1}$

$$m_{ab} = m_f * A \tag{22}$$

Mathematical model is developed for the falling film flowing on horizontal round tubes absorber derived from the mathematical model of the control volume element. The control volume element is simplified into two-dimensional physical model in many previous studies. Cooling tube diameter is 9.6 mm. The liquid mass flow rate per unit length of tube is low to get droplet mode.

### 3 RESULT AND DISCUSSION

#### 3.1 Numerical validation

The parameters used in this study are presented in table 1 [10].

Table 1: Input parameters

Parameters	Values
Inlet solution temperature $T_{in}$	316.15 K
Inlet solution concentration $\omega_{in}$	0.295
Absorber pressure $p$	2 bar
Solution density	$880 \text{ kg m}^{-3}$
Dynamic viscosity $\mu$	$3.958 * 10^{-4} \text{ N s m}^{-2}$
Solution flow rate $\Gamma$	$0.005 \text{ kg m}^{-1} \text{ s}^{-1}$
Out tube radius $R_o$	0.005 m
Thermal diffusivity $\alpha$	$6.7 * 10^{-8} \text{ m}^2 \text{ s}^{-1}$
Mass diffusivity $D$	$4.4 * 10^{-9} \text{ m}^2 \text{ s}^{-1}$
Wall tube temperature $T_{wall}$	303.15 K
Thermal conductivity of solution $k_f$	$0.384 \text{ W m}^{-1} \text{ K}^{-1}$

Figure 4 shows the mass transfer phenomenon as NH<sub>3</sub> vapor is absorbed in order to become a stronger concentration solution of a control volume element.

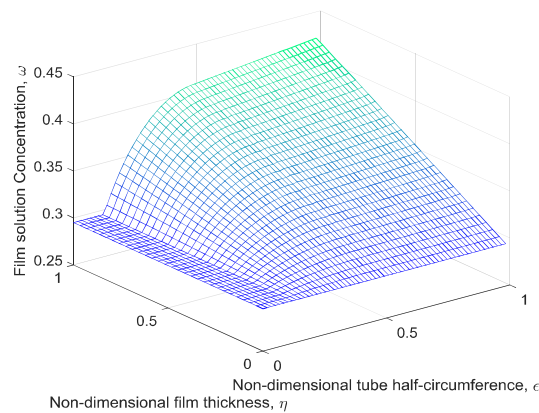


Figure 4: Concentration profile,  $\omega$

Figure 4 is the three-dimensional distribution of the concentration  $\omega$  in the solution film domain of a control volume element. Concentration of dilute solution when the solution has not contact the tube assumed without absorption phenomenon so the concentration equals the inlet concentration. Interface temperature is saturated to solution concentration. At tube wall, solution temperature equals wall temperature. When absorption phenomenon occurs, concentration of the liquid-vapor interface increases along  $\epsilon$ -axis ( $x$ ), then diffuses into the tube wall along  $\eta$ -axis ( $y$ ). This absorption generates heat making liquid-vapor interface

temperature increases along  $\varepsilon$ -axis ( $x$ ). Due to the temperature difference between the interface and tube wall, heat transfer to the wall along axis  $\eta$  ( $y$ ).

Average concentration of the film leaves the wall  $\omega = 0.3537$ ; increases 0.0587. Average temperature of the film coming in the tube is 317.6 K (44.5 °C), average temperature of the film leaving tube is  $T = 304.8$  K (31.7 °C), decreases 12.8 °C. Temperature of the liquid-vapor interface coming in the tube is 332 K (58 °C), temperature of the liquid-vapor interface leaving the tube is  $T = 306.5$  K (33.4 °C), decreased 24.7 °C. Difference temperature between liquid-vapor interface leaving the tube and the tube wall is 3.4 °C. Simulations based on the geometry structure and operating conditions of the absorber in the machine. The cooling tube bundle is arranged in 28 parallel rows (8 pass). Each row has an area of  $A_1 = \pi * D_o * l * n = \pi * 0.0096 * 0.18 * 6 = 0.0326$  m<sup>2</sup>. The following figures show the heat and mass transfer process in the absorber. Typical values when absorption refrigeration machine operates in ice-making mode with the weak solution flow rate is 0.0171 kgs<sup>-1</sup> or  $\Gamma = 0.008$  kgm<sup>-1</sup>s<sup>-1</sup>; the weak solution inlet  $\omega = 29\%$ ; the inlet and outlet of cooling water temperature are 31 °C and 34.2 °C respectively.

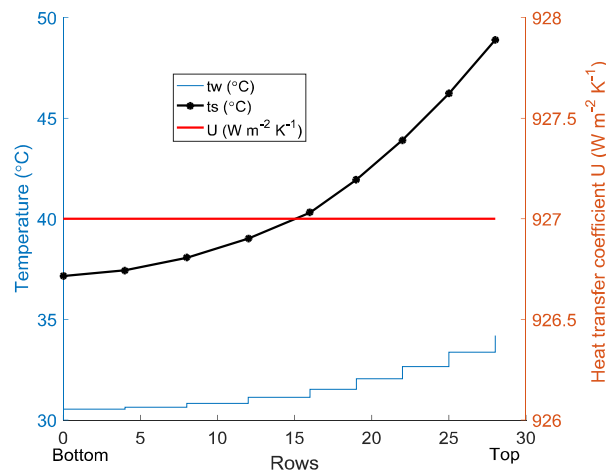


Figure 5: Variation of temperature & heat transfer coefficient

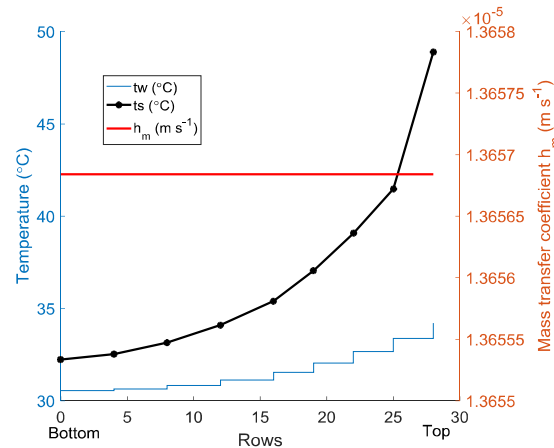


Figure 6: Variation of temperature & mass transfer coefficient

Figure 5 shows the variation of the solution average temperature, water coolant along the horizontal tube-type falling film absorber design. The solution flows down from the top of the absorber (28 tube rows) to the bottom of the absorber. While water coolant flows in the upward direction. The heat transfer coefficient is approximately constant  $U = 927$  Wm<sup>-2</sup>K<sup>-1</sup>. The mass transfer coefficient is approximately constant  $h_m =$

$1.3657 \times 10^{-5} \text{ ms}^{-1}$  (Figure 6).

### 3.2 Evaluation of numerical and experimental result

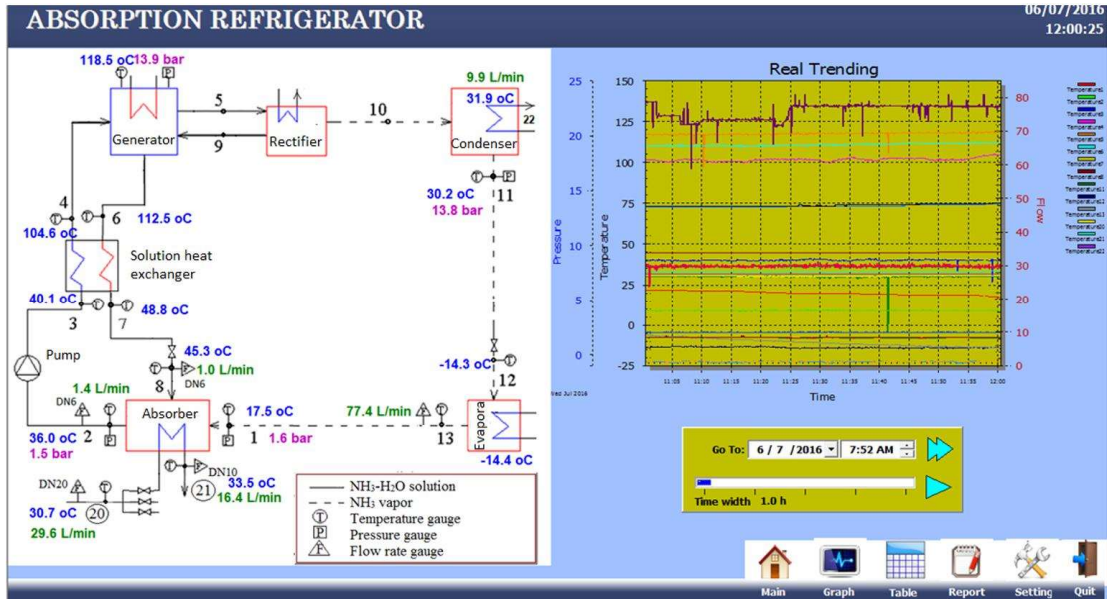


Figure 7: Measured state point values

Figure 7 shows the measured state point values for a specific working condition. The measured value of absorber heat load  $Q_{a\_meas} = 3.270 \text{ kW}$  is compared with the computed value  $Q_{a\_compute}$  and numerical model  $Q_{a\_sim}$ . The input for the machine computation program are the condensing temperature  $t_c = 30.2 \text{ oC}$ , absorbing temperature of strong solution leaving the absorber  $t_a = 36 \text{ oC}$ , evaporating temperature  $t_e = -19 \text{ oC}$ , and the heat supply capacity  $Q_g = 3.762 \text{ kW}$ . The optimal generating temperature will be  $t_g = 120 \text{ }^\circ\text{C}$ . Heat flows of the components: evaporator, condenser, absorber, generator, rectifier, work input to the solution pump, coefficient of performance are  $Q_e = 1.52 \text{ kW}$ ;  $Q_c = 1.727 \text{ kW}$ ;  $Q_a = 3.412 \text{ kW}$ ;  $Q_g = 3.762 \text{ kW}$ ;  $Q_r = 0.41 \text{ kW}$ ;  $Q_{p\_out} = 0.362 \text{ kW}$ ;  $\text{COP} = 0.413$  respectively. The heat load of the absorber  $Q_{a\_compute} = 3.412 \text{ kW}$ .

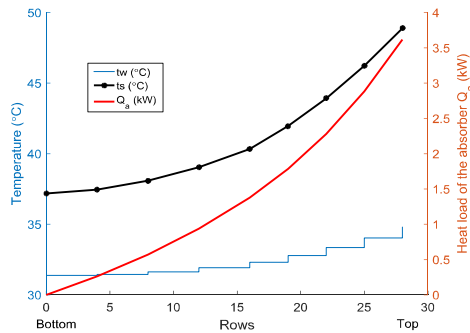


Figure 8: Variation of temperature and heat load

Figure 8 shows the variation of the simulated value of absorber  $Q_{a\_sim} = 3.671 \text{ kW}$ , the solution average temperature  $t_s$ , water coolant  $t_w$  along the horizontal tube-type falling film absorber design. While water coolant flows in the upward direction. The heat transfer coefficient is approximately constant  $U = 863 \text{ Wm}^{-2}\text{K}^{-1}$ .

Table 2: Numerical and experimental heat load of the absorber

Head load	Value (kW)	Deviation (%)
$Q_{a\_meas}$	3.270	0
$Q_{a\_compute}$	3.412	4.3
$Q_{a\_sim}$	3.671	12.3

The heat transfer coefficient and mass transfer coefficient as functions of the initial solution concentration, solution mass flow rate per unit tube length, and cooling water temperature are derived as  $U = f(\omega; \Gamma; T) = f(0.308; 0.008; 306.3) = 0.863 \text{ kWm}^{-2}\text{K}^{-1}$ ;  $h_m = f(\omega; \Gamma; T) = f(0.308; 0.008; 306.3) = 1.45 \cdot 10^{-5} \text{ ms}^{-1}$  respectively.

Table 3: Comparison of heat and mass transfer coefficient with other literatures

Analysis	$U \text{ Wm}^{-2}\text{K}^{-1}$	$h_m \text{ ms}^{-1}$	Note
[14]	545-940		$D_o = 1.575$ ; $D_i = 1.168$ . $m = 0.0151 \div 0.0266$ , $t = 52 \text{ \& } 81$ ; $\omega = 28 \div 35$ .
[15]	540-1160		$D_o = 1.575$ ; $D_i = 1.168$ $\Gamma = 0.00138 \div 0.005$ or $m = 0.0189 \div 0.0284$
[16]	571-831	$2.1944 \cdot 10^{-5} \div 3.2222 \cdot 10^{-5}$	$D_o = 15.88$ or $12.7$ or $9.52$ Sim. $\Gamma = 0.008 \div 0.05$ Exp. $\Gamma = 0.0143 \div 0.0303$
[17]	852	$m_f = 0.01453$ $m_f = 0.01847$	$m = 0.0095 \div 0.0191$ or $\Gamma = 0.03 \div 0.06$ ; $t = 39.8 \div 49.7$ ; $\omega = 39.6\%$ .
[18]	753-1853	$0.55 \cdot 10^{-5} \div 3.31 \cdot 10^{-5}$	$D_o = 9.5$
Present study	488 $\div$ 976	$0.967 \cdot 10^{-5} \div 1.65 \cdot 10^{-5}$	$\omega = 30\%$ ; $T_w = 306.3 \text{ K}$ ; $\Gamma = 0.001 \div 0.03$

In addition, heat transfer and mass transfer coefficients of this research are compared with previous studies. Sangsoo Lee, Lalit Kumar Bohra, Srinivas Garimella, Ananda Krishna Nagavarapu [18] found heat transfer coefficient  $U = f(C; \Gamma; P) = f(0.25; 0.008; 2.5) = 0.88 \text{ kWm}^{-2}\text{K}^{-1}$  and mass transfer coefficient  $h_m = f(C; \Gamma; P) = f(0.25; 0.008; 2.5) = 1.65 \cdot 10^{-5} \text{ ms}^{-1}$ . Correlations of heat transfer and mass transfer coefficients of the absorption process to: (i) solution concentration ranging from 28% to 31%, (ii) solution mass flow rate per unit tube length ranging from  $0.001 \text{ kgm}^{-1}\text{s}^{-1}$  to  $0.03 \text{ kgm}^{-1}\text{s}^{-1}$  and (iii) cooling water temperature ranging from 301 K to 311 K were established.

### 3.3 Correlation of heat and mass transfer coefficients

The effects of the solution concentration, solution mass flow rate per unit tube length, and cooling water temperature to the heat transfer coefficient and mass transfer coefficient in the absorption process.

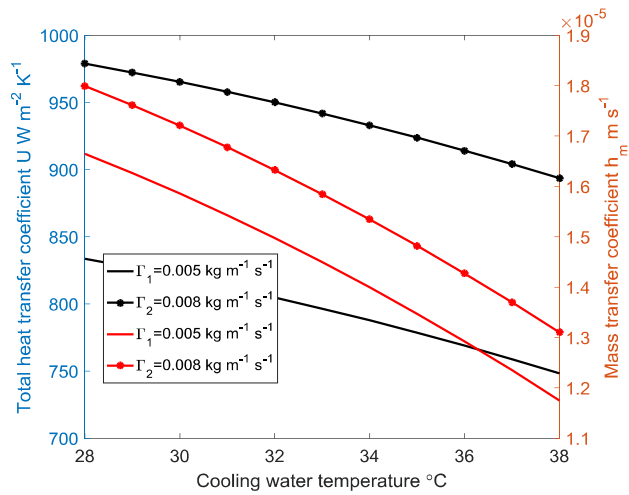


Figure 9: Effect of cooling water temperature on U and  $h_m$

The cooling water temperature decreases 1 °C the heat transfer coefficient increase 0.95% and mass transfer coefficient increase 3.7%. Figure 9 also shows the combined effects of the cooling water temperature variation and solution mass flow rate per unit length.

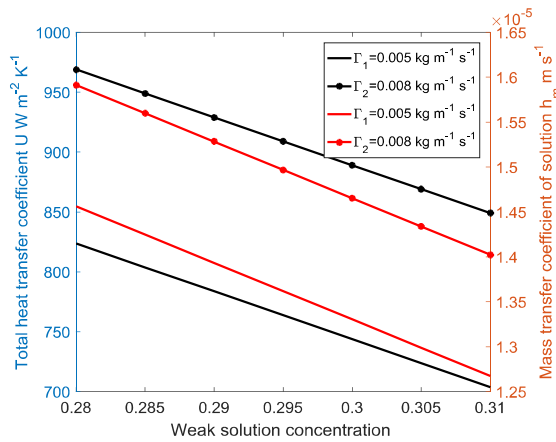
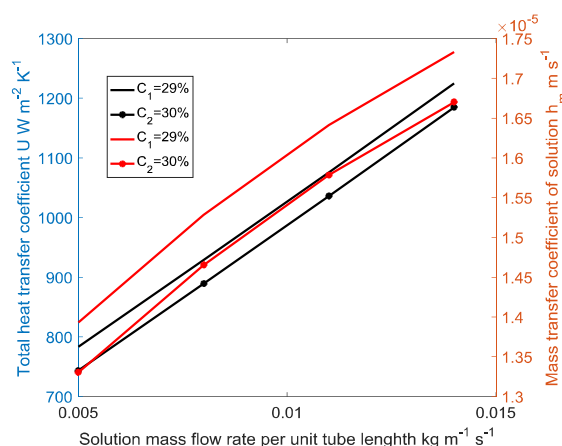


Figure 10: Effect of solution concentration on U and  $h_m$

The solution concentration decreases 1%, the heat transfer coefficient increase 1.46% and mass transfer coefficient increase 1.39% (figure 10).

Figure 11: Solution distribution on U and  $h_m$ 

The solution mass flow rate per unit tube length decreases 1%, the heat transfer coefficient increase 0.65% and mass transfer coefficient increase 3.27% (figure 11).

A correlation which gives the heat transfer coefficient and mass transfer coefficient in the absorption process in range of solution concentration  $\omega = 28 \div 31$  (%), solution mass flow rate per unit tube length  $\Gamma = 0.005 \div 0.015$  ( $\text{kgm}^{-1}\text{s}^{-1}$ ), coolant temperature  $t = 28 \div 38$  ( $^{\circ}\text{C}$ ) are set as two functions.

These functions are derived to estimate the overall heat transfer coefficient U and mass transfer coefficient of NH<sub>3</sub> vapor into NH<sub>3</sub>-H<sub>2</sub>O solution  $h_m$  taking the form as function (23) from the results of the individual studies on the effects of heat and mass transfer of related studies and assumptions limiting the operating conditions of absorber.

$$U \text{ or } h_m = A + B*\omega + C*\Gamma + D*T_{\text{wall}} + G*\Gamma^2 + K*T_{\text{wall}}^2 \quad (23)$$

Table 4: Constant of U and  $h_m$  correlation

Constant	U $\text{Wm}^{-2}\text{K}^{-1}$	$h_m \text{ms}^{-1}$
A	-16374,2444	-0.0009451752
B	-3999,9999	-0.0000629999
C	47142,4463	0.0006066080
D	126,7608	0.00000686285
G	97578,4861	-0.0120566076
K	-0,2211	-0.0000000120

#### 4 CONCLUSION

The effects of the solution concentration, solution mass flow rate per unit tube length, and cooling water temperature to the heat transfer coefficient and mass transfer coefficient in the absorption process are given by table 5.

Table 5: The effects on U and  $h_m$ 

Variable	U $\text{W m}^{-2}\text{K}^{-1}$	$h_m \text{ms}^{-1}$
$\Gamma$ decrease 1%	decrease 0.56 %	decrease 3.27%
$t_w$ decrease 1 $^{\circ}\text{C}$	increase 0.95%	increase 3.7%
$\omega$ decrease 1%	increase 1.46%	increase 1.39%

The correlation which give the heat transfer coefficient and mass transfer coefficient in the absorption

process in range of solution concentration  $\omega = 28 \div 31$  (%), solution mass flow rate per unit tube length  $\Gamma = 0.005 \div 0.015$  kgm<sup>-1</sup>s<sup>-1</sup>, coolant temperature  $t = 28 \div 38$  (°C) are set as function 23.

## REFERENCES

- [1] Nomura, T., N. Nishimura, S. Wei and S. Yamaguchi. Heat and Mass Transfer Mechanism in the Absorber of H<sub>2</sub>O/LiBr Conventional Absorption Refrigerator: Experimental Examination by Visualized Model, *International Absorption Heat Pump Conference*, AES–vol. 31, pp.203–208. 1993.
- [2] Islam, M.R., N.E. Wijesundera and J.C. Ho. Simplified models for coupled heat and mass transfer in falling-film absorbers, *Int. J. of Heat and Mass Transfer.*, vol. 47(2), pp. 395-406. 2004
- [3] Oosthuizen, Patric H. and David Naylor. Edwards, *Convective Heat Transfer Analysis*, pp. 5756-577, *McGraw-Hill International Editions*, 1999.
- [4] Islam, M.R., N.E. Wijesundera and J.C. Ho. Simplified models for coupled heat and mass transfer in falling-film absorbers, *Int. J. of Heat and Mass Transfer*, vol. 47(2), pp. 395-406, 2004.
- [5] Hu, X. and A.M. Jacobi. Departure-site spacing for liquid droplets and jets falling between horizontal circular tubes, *Experimental Thermal and Fluid Science*, Vol. 16, p. 322-331, 1998.
- [6] Killion, J.D. and S. Garimella. Gravity-driven Flow of Liquid Films and Droplets in Horizontal Tube Banks, *International Journal of Refrigeration*, vol. 26, p. 516-526, 2003.
- [7] Frances, V.M.S. and J.M.P. Ojer. Validation of a Model for the Absorption Process of H<sub>2</sub>O (vap.) By a LiBr(aq.) in a Horizontal Tube Bundle, Using Multi-factorial Analysis, *International Journal of Heat and Mass Transfer*, vol.46(17), pp.3299-3312. 2003.
- [8] Islam, M.R., N.E. Wijesundera and J.C. Ho. Evaluation of Heat and Mass Transfer Coefficients for Falling-Films on Tubular Absorbers, *Int. J. Refrigeration*, vol. 26, p. 197-204, 2003.
- [9] Jesse D. Killion, Srinivas Garimella. Pendant droplet motion for absorption on horizontal tube banks. *International Journal of Heat and Mass Transfer* 47 p. 4403–4414, 2004.
- [10] Conlisk AT, Mao J, “Nonisothermal absorption on a horizontal cylindrical tube-1. The film flow”, *Chemical engineering science*, 51, p. 1275-1285, 1996.
- [11] Md. Raisul Islam, “Absorption process of a falling film on a tubular absorber: An experimental and numerical study”, *Applied Thermal Engineering* 28, p. 1386–1394, 2008.
- [12] V.D. Papaefthimiou, I.P. Koronaki, D.C. Karampinos, E.D. Rogdakis, “A novel approach for modelling LiBr- H<sub>2</sub>O falling film absorption on cooled horizontal bundle of tubes”, *Int. J. of refrigeration* 35, p. 1115-1122, 2012.
- [13] L. Harikrishnan, Shaligram Tiwari\*, M.P. Maiya, “Numerical study of heat and mass transfer characteristics on a falling film horizontal tubular absorber for R-134a-DMAC”, *International Journal of Thermal Sciences* 50, p. 149-159, 2011.
- [14] Meacham, J.M.G., Srinivas, Ammonia-Water Absorption Heat and Mass Transfer in Microchannel Absorbers with Visual Confirmation. *ASHRAE 2004*. **110** (1): p. 525-532.
- [15] Garimella, S., et al., Microchannel component technology for system-wide application in ammonia/water absorption heat pumps. *International Journal of Refrigeration*, 2011. **34**(5): p. 1184-1196.

- [16] Phan, T.T., Performance of Horizontal Tube Absorber with Variation of Tube Diameter. 2007, *Pukyong National University*.
- [17] Islam, M.R., N.E. Wijesundera, and J.C. Ho, Evaluation of heat and mass transfer coefficients for falling-films on tubular absorbers. *International Journal of Refrigeration*, 2003. **26**(2): p. 197-204.
- [18] Lee, S., et al., Measurement of absorption rates in horizontal-tube falling-film ammonia-water absorbers. *International Journal of Refrigeration*, 2012. **35**(3): p. 613-632.

Ngày gửi bài: 06/01/2020

Ngày chấp nhận đăng: 29/04/2020

## CÁC THÔNG SỐ ẢNH HƯỞNG ĐẾN SỰ TRUYỀN NHIỆT – TRUYỀN CHẤT CỦA DUNG DỊCH CHẢY TRÊN ỐNG TRÒN NẰM NGANG

**Tóm tắt.** Quá trình hấp thụ được xem là quá trình quang trọng nhất trong các máy lạnh hấp thụ về phương diện nâng cao hiệu suất tổng của máy. Một trong những hướng nghiên cứu mấu chốt là chọn lựa được cấu trúc bộ hấp thụ phù hợp với điều kiện chế tạo tại Việt Nam, không cần đầu tư cơ sở hạ tầng mới. Ở nghiên cứu này, một mô hình cục bộ của sự truyền nhiệt – truyền chất kết hợp trong quá trình hấp thụ hơi NH<sub>3</sub> vào dung dịch NH<sub>3</sub>-H<sub>2</sub>O loãng chảy trên các ống tròn nằm ngang của bộ hấp thụ được thực hiện. Hệ số truyền nhiệt tìm được từ mô hình toán truyền nhiệt – truyền chất kết hợp. Hệ số truyền nhiệt được sử dụng để tính giá trị mô phỏng của tải nhiệt. Hệ số truyền nhiệt, hệ số truyền chất trong quá trình truyền nhiệt tìm được trong phạm vi nồng độ dung dịch  $\omega = 28\% \div 31\%$ , lưu lượng khối lượng theo chiều dài  $\Gamma = 0.001 \div 0.03 \text{ kgm}^{-1}\text{s}^{-1}$ , nhiệt độ nước giải nhiệt  $t_{\text{water}} = 28 \text{ oC} \div 38 \text{ oC}$  được thiết lập thành hai hàm số. Sự giảm tỉ lệ ướt bề mặt theo các phân tích được đưa vào tính khi dòng dung dịch chảy từ đỉnh xuống đáy của chùm ống song song. Sai số giữa tải nhiệt theo lý thuyết và theo thực nghiệm khoảng 12.3%. Dựa trên những mô phỏng này, các nghiên cứu lý thuyết được thực hiện cho hệ thống lạnh hấp thụ để giới hạn phạm vi thực hiện thí nghiệm. Kết quả của nghiên cứu này là cơ bản cho các nghiên cứu ứng dụng tiếp theo của các bộ hấp thụ dạng màng.

**Từ khóa.** quá trình hấp thụ, Dung dịch NH<sub>3</sub>-H<sub>2</sub>O, làm lạnh hấp thụ